2872 *Inorg. Chem.* **2010**, *49*, 2872–2880
DOI: 10.1021/ic902444x

Inorganic Chemistry
Article

Synthesis of a Novel Sn(IV) Porphycene−Ferrocene Triad Linked by Axial Coordination and Solvent Polarity Effect in Photoinduced Charge Separation Process

Daisuke Maeda,[†] Hisashi Shimakoshi,[†] Masaaki Abe,[†] Mamoru Fujitsuka,[‡] Testuro Majima,[‡] and Yoshio Hisaeda*,[†]

[†]*Department of Chemistry and Biochemistry, Graduate School of Engineering, Kyushu University, Fukuoka 819-0395, Japan, and* [‡]*Institute of Scientific and Industrial Research (SANKEN), Osaka University, Mihogaoka 8-1, Ibaraki, Osaka 567-0047, Japan*

Received December 9, 2009

A novel Sn(IV) porphycene−ferrocene triad molecule, *trans*-bis(ferrocenecarboxylato)(2,3,6,7,12,13,16,17-octaethylporphycenato)tin(IV), [Sn^{IV}(OEPc)($FcCOO)_2$] (**2**), was synthesized and fully characterized by various spectroscopic methods. This is the first example of a metalloporphycene triad linked by the axial coordination of two functionalized units to a metallocenter. The steady-state fluorescence measurement indicated the efficient fluorescence quenching by coordination of the ferrocenecarboxylic acid in comparison to the corresponding dihydroxy−Sn(IV) porphycene, [Sn^{IV}(OEPc)($OH)_2$] (**1**) (**1**, $\Phi_F = 0.094$; **2**, $\Phi_F = 0.01$). The electron transfer process from the ferrocene units to the excited Sn(IV) porphycene was directly observed by subpicosecond transient absorption spectroscopy in acetonitrile (polar solvent) and toluene (nonpolar solvent). In acetonitrile, the transient species attributed to the Sn(IV) porphycene radical anion was observed at 750 and 850 nm within 1 ps after the excitation, and then the generated charge separation state disappeared with a value of 6.9×10^{11} s^{-1} for the time constant. On the other hand, the generated charge separation state decayed with two components, 3.9×10^{11} and 9.6×10^9 s^{-1} time constants, in toluene. For the observed two-component decay in toluene, a significant equilibrium between the charge separation state and the triplet state was proposed because these energy levels are close to each other. Therefore, the solvent-polarity-dependent long-lived charge separation state was obtained in the Sn(IV) porphycene−ferrocene triad system. The electron transfer upon excitation of the Sn(IV) porphyrin of [Sn^{IV}(OEP)-($FcCOO)_2$] (**4**), in which OEP denotes the 2,3,6,7,12,13,16,17-octaethylporphyrin ligand, was observed. However, no equilibrium between the charge separation and the triplet states was observed in both the acetonitrile and toluene. The difference in the charge recombination processes of the Sn(IV)−porphycene and −porphyrin is due to the small HOMO−LUMO gap and the large driving force ($-\Delta G_{CS}$) of **2** compared to that of **4**, which resulted in the energy level of the charge separation state close to the triplet state in toluene. Furthermore, the large driving force ($-\Delta G_{CS}$) of **2** compared to that of **4** is attributed to the significant stabilization of the LUMO energy level caused by a decrease in the molecular symmetry and a large porphycene π-electron framework. This result indicates that porphycenes are excellent candidates as an electron acceptor in photoinduced electron transfer systems.

Introduction

The design and development of novel artificial photosynthesis in molecular electronic devices are sincerely desired. A number of such molecular devices consist of porphyrins due to their potential application as electron donors in the photoinduced electron transfer (PET) reaction of photosynthetic models.[1] Thus, inspired by the significance of the porphyrins, a new research direction devoted to the preparation and study of nonporphyrin tetrapyrrolic macrocycles has emerged.[2] Over the past two decades, many porphyrin isomers have been reported.[3] Porphycene is also one of the artificial tetrapyrrole ligands, and this ligand was first

*To whom correspondence should be addressed. E-mail: yhisatcm@mail.cstm.kyushu-u.ac.jp.

(1) (a) Wasielewski, M. R. *Chem. Rev.* **1992**, *92*, 435. (b) Kadish, K. M.; Smith, K. M. Guilard, R. In *The Porphyrin Handbook*; Elsevier: New York, 1999; vols. *16*−*19*. (c) Fukuzumi, S.; Honda, T.; Ohkubo, K.; Kojima, T. *Dalton Trans.* **2009**, 3880.

(2) (a) Sessler, J. L.; Weghorn, S. J. In *Expanded, Contracted & Isomeric Porphyrins*; Pergamon: New York, 1997. (b) Vogel, E. *Pure Appl. Chem.* **1990**, *62*, 557. (c) Kadish, K. M.; Smith, K. M. Guilard, R. In *The Porphyrin Handbook*; Elsevier: New York, 1999; vol. *15*.

(3) (a) Kadish, K. M.; Smith, K. M. Guilard, R. In *The Porphyrin Handbook*; Elsevier: New York, 1999; vol. *8*. (b) Fowler, C. J.; Sessler, J. L.; Lynch, V. M.; Wauluk, J.; Gebauer, A.; Lex, J.; Zuniga-y-Rivero, F.; Vogel, E. *Chem.—Eur. J.* **2002**, *8*, 3485. (c) Furuta, H.; Asano, T.; Ogawa, T. *J. Am. Chem. Soc.* **1994**, *116*, 767.

 Published on Web 02/15/2010 © 2010 American Chemical Society

synthesized by Vogel et al.[4−6] It is known that several interesting photochemical properties attributed to its ring-framework modification can be realized.[7] These photochemical properties have been elucidated on the basis of structural, theoretical, and electrochemical studies.[8−13] For example, these porphyrin isomers have a small HOMO−LUMO gap and stronger absorption bands than those of the porphyrins in the visible region by symmetry reduction from D_{4h} to D_{2h}. Therefore, porphycenes are very attractive and excellent candidates for PET.

Recently, several PET reactions for porphycene and metalloporphycene have been reported.[14] We investigated the PET processes of Zn octaethylporphycene using transient absorption spectroscopy in which the transient absorption bands of the radical cation of porphycene and the radical anion of the acceptor were directly observed.[15] D'Souza et al. reported the noncovalently linked electron donor−acceptor system consisting of Zn porphycene as the donor and the pyridine appended C_{60} as the acceptor, and efficient quenching of the Zn-porphycene emission indicating PET was confirmed by axial coordination of the pyridine appended C_{60}.[16] Levanon and his co-worker investigated the PET reaction between the excited triplet state of the free-base or Zn-coordinated porphycene and duroquinone and reported the formation of the duroquinone radical anion by time-resolved EPR.[17] Also, Nonell et al. reported the generation of the radical anion and cation species of the free-base and of its Pd−tetraphenylporphycene by photochemical methods.[18] Although the intramolecular PET reactions of the porphycene derivative as an electron donor have been investigated in these previous studies, there is only one example which reported PET studies of a supramolecular system consisting of a porphycene derivative as an electron acceptor to the best of our knowledge.[19] Sessler, Kadish, and Fukuzumi et al. synthesized the fused compounds of a ruthenocene complex onto the metalloporphycene π-electron framework and reported the photoinduced electron transfer from the ruthenocene moiety to the singlet excited state of the metalloporphycene.

Chart 1. Chemical Structures of Sn(IV) Complexes

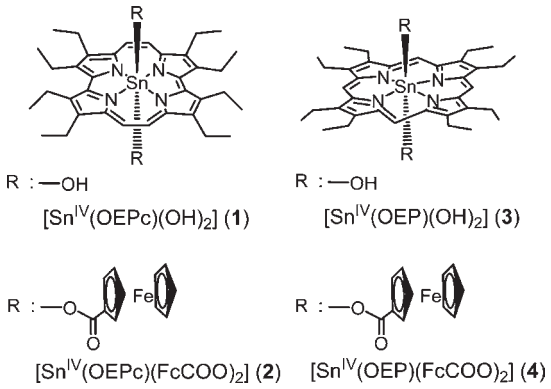

In the present study, we focused on the PET reaction of the triad structure, **2**, consisting of Sn(IV) octaethylporphycene, [Sn^{IV}(OEPc)], as the acceptor and ferrocenecarboxylic acid, FcCOO, as the donor (Chart 1). Among the several methods developed to construct the donor−acceptor system, axial ligation to the central metal ion of the metalloporphyrins using functionalized donor/acceptor molecules is commonly used. Also, it is known that the Sn(IV) complexes with six-coordinate carboxylate and aryloxide axial anions are readily prepared due to the oxophilic nature of the Sn(IV) center, making the building blocks for construction of the elaborate arrays.[20,21] Nevertheless, the PET behavior of porphycene triads linked by an axial coordination has not yet been explored. Therefore, we have been interested in a PET system based on the Sn(IV) porphycene. This is the first example of a porphycene triad linked by the axial coordination of two functionalized donor units to a metalloporphycene. Herein, the crystal structures of the Sn(IV)−ferrocene complexes were elucidated, and the PET processes from FcCOO to [Sn^{IV}(OEPc)] were mainly investigated by subpicosecond transient absorption spectroscopy. The formation of the porphycene radical anion species in the charge separation (CS) state was successfully confirmed by observing the transient absorption bands during the laser flash photolysis. Furthermore, the PET process of the Sn(IV) porphycene was compared to the corresponding Sn(IV) porphyrin, **4**, having the same equatorial substituent and axial ligands. On the basis of these results, the unique characteristic properties of porphycene ligands and differences between the porphycene and porphyrin ligands due to the skeleton change were investigated.

Experimental Section

Chemicals. For the UV−vis, fluorescent spectroscopy, and the transient absorption spectrum studies, spectroscopic grade toluene, acetonitrile, and dichloromethane were purchased from DOJINDO (Japan) and KISHIDA (Japan). For the syntheses of **2** and **4**, dichloromethane was stirred for one day in the

(4) Vogel, E.; Köcher, M.; Schmickler, H.; Lex, J. *Angew. Chem., Int. Ed.* **1986**, *25*, 257.
(5) Vogel, E.; Bröring, M.; Weghorn, S. J.; Scholz, P.; Deponte, R.; Lex, J.; Schmickler, H.; Schaffner, K.; Braslavsky, S. E.; Müller, M.; Pörting, S.; Fowler, C. J.; Sessler, J. L. *Angew. Chem., Int. Ed.* **1997**, *36*, 1651.
(6) Sánchez-García, D.; Sessler, J. L. *Chem. Soc. Rev.* **2008**, *37*, 215.
(7) (a) Shimakoshi, H.; Baba, T.; Iseki, Y.; Endo, A.; Adachi, C.; Hisaeda, Y. *Chem. Commun.* **2008**, 2882. (b) Baba, T.; Shimakoshi, H.; Endo, A.; Adachi, C.; Hisaeda, Y. *Chem. Lett.* **2008**, *37*, 264. (c) Maeda, D.; Shimakoshi, H.; Abe, M.; Hisaeda, Y. *Dalton Trans.* **2009**, 140. (d) Maeda, D.; Shimakoshi, H.; Abe, M.; Hisaeda, Y. *Inorg. Chem.* **2009**, *48*, 9853.
(8) Nonell, S.; Aramendia, P. F.; Heihoff, K.; Negri, R. M.; Braslavsky, S. E. *J. Phys. Chem.* **1990**, *94*, 5879.
(9) Waluk, J.; Müller, M.; Swiderek, P.; Köcher, M.; Vogel, E.; Hohlneicher, G.; Michl, J. *J. Am. Chem. Soc.* **1991**, *113*, 5511.
(10) Hasegawa, J.; Takata, K.; Miyahara, T.; Neya, S.; Frisch, M. J.; Nakatsuji, H. *J. Phys. Chem. A.* **2005**, *109*, 3187.
(11) Gil, M.; Waluk, J. *J. Am. Chem. Soc.* **2007**, *129*, 1335.
(12) Fita, P.; Radzewicz, C.; Waluk, J. *J. Phys. Chem. A.* **2008**, *112*, 10753.
(13) Fita, P.; Urbańska, N.; Radzewicz, C.; Waluk, J. *Chem.—Eur. J.* **2009**, *15*, 4851.
(14) (a) Guldi, D. M.; Neta, P.; Vogel, E. *J. Phys. Chem.* **1996**, *100*, 4097. (b) Guldi, D. M.; Field, J.; Grodkowski, J.; Neta, P.; Vogel, E. *J. Phys. Chem.* **1996**, *100*, 13609.
(15) Fujitsuka, M.; Shimakoshi, H.; Tojo, S.; Cheng, L.; Maeda, D.; Hisaeda, Y.; Majima, T. *J. Phys. Chem. A.* **2009**, *113*, 3330.
(16) D'Souza, F.; Deviprasad, G. R.; Rahman, M. S.; Choi, J.-P. *Inorg. Chem.* **1999**, *38*, 2157.
(17) Berman, A.; Michaeli, A.; Feitelson, J.; Bowman, M. K.; Norris, J. R.; Levanon, H.; Vogel, E.; Koch, P. *J. Phys. Chem.* **1992**, *96*, 3041.
(18) Rubio, N.; Borrell, J. I.; Teixidó, J.; Cañete, M.; Juarranz, Á.; Villanueva, Á.; Stockert, J. C.; Nonell, S. *Photochem. Photobiol. Sci.* **2006**, *5*, 376.
(19) Cuesta, L.; Karnas, E.; Lynch, V. M.; Chen, P.; Shen, J.; Kadish, K. M.; Ohkubo, K.; Fukuzumi, S.; Sessler, J. L. *J. Am. Chem. Soc.* **2009**, *131*, 13538.
(20) (a) Slagt, V. F.; van Leeumen, P. W. N. M.; Reek, J. N. H. *Dalton Trans.* **2007**, 2302. (b) Arnold, D. P.; Blok, J. *Coord. Chem. Rev.* **2004**, *248*, 299.
(21) (a) Kim, H. J.; Jang, J. H.; Choi, H.; Lee, T.; Ko, J.; Yoon, M.; Kim, H.-J. *Inorg. Chem.* **2008**, *47*, 2411. (b) Kim, Y.; Mayer, M. F.; Zimmerman, S. C. *Angew. Chem., Int. Ed.* **2003**, *42*, 1121.

presence of calcium hydrate under a nitrogen atmosphere, then distilled under a nitrogen atmosphere and used immediately.

Measurements. The elemental analyses were done at the Service Center of Elementary Analysis of Organic Compounds of Kyushu University. The ^{1}H NMR spectra were recorded by a Bruker Avance 500 spectrometer installed at the Center of Advanced Instrumental Analysis of Kyushu University, and the chemical shifts (in ppm) were referenced relative to the residual protic solvent peak. The UV−vis absorption spectra were measured using a Hitachi U-3300 spectrophotometer at room temperature. The fluorescence spectra were measured by a HITACHI Fluorescence Spectrophotometer F-4500 at room temperature. The MALDI-TOF mass spectra were obtained using a Bruker Autoflex II without the matrix. The electrospray ionization (ESI) mass spectra were obtained using a JMS-T100CS AccuTOF. For the theoretical study, the optimized structures were determined from the X-ray analysis data, and then the HOMO and LUMO orbitals of **2** and **4** were estimated at the B3LYP/3-21G* level using the Gaussian 03 package.[22]

Electrochemical Measurements. The cyclic voltammograms (CV) were obtained using a BAS ALS model 630c electrochemical analyzer. A three-electrode cell equipped with a 1.6-mm-diameter platinum wire as the working and counter electrodes was used. A Ag−AgCl (3.0 M NaCl) electrode served as the reference. A nonaqueous dichloromethane solution containing **2** or **4** (1.0×10^{-3} M) and tetra-*n*-butylammonium hexafluorophosphate ($TBAPF_6$; 1.0×10^{-1} M) was deaerated prior to each measurement, and a nitrogen atmosphere was maintained inside the cell throughout each measurement. All measurements were carried out at room temperature.

Photophysical Measurements. The fluorescence quantum yield (Φ_f) value of **1** was measured using an absolute photoluminescence quantum efficiency measurement system (Hamamatsu C9920−02) incorporating an integrating sphere. To measure Φ_f, a degassed solution of **1** in toluene was prepared and the concentration was adjusted so that the absorbance of the solution at 337 nm would be less than 0.1. The excitation was performed at 337 nm. In contrast, the determined Φ_f values of **2**, **3**, and **4** are less than 3% in this method. For the absolute photoluminescence quantum efficiency measurement, the values less than 3% are not correct values from the viewpoint of sensitivity of the instruments. Therefore, the Φ_f values of **2**, **3**, and **4** were determined by the comparative method reported by Williams et al., in which 2,7,12,17-tetra-*n*-propyl porphycene was used as the standard.[23] The solutions of the standard and test sample, **2**, **3**, and **4** with identical absorbances at the same excitation wavelength can be assumed to be absorbing the same number of photons. Thus, a simple ratio of the integrated fluorescence intensities of both solutions will afford the ratio of the quantum yield values (Figure S1, Supporting Information). To measure Φ_f using this method, degassed solutions of **2**, **3**, and **4** in toluene were prepared and the concentration was also adjusted so that the absorbance of the solution at 337 nm would be 0.10. The excitation was performed at 337 nm.

The subpicosecond transient absorption spectra were measured by the pump and probe method using a regeneratively amplified titanium sapphire laser as previously reported.[24] In the present study, the sample was excited using a 620 or 540 nm laser pulse, which was generated by an optical parametric amplifier. For the transient absorption measurements, the concentration was adjusted so that the absorbance of the solution at 620 or 540 nm would be 0.5 in a cell with 1.0 mm of optical path length.

Syntheses. *trans*-Dichloro(2,3,6,7,12,13,16,17-octaethylporphyrinato)tin(IV) [Sn^{IV}(OEP)Cl_2] and *trans*-dichloro(2,3,6,7,12,13,16,17-octaethylporphycenato)tin(IV) [Sn^{IV}(OEPc)Cl_2] were synthesized according to the reported procedures.[7d,25]

***trans*-Dihydroxo(2,3,6,7,12,13,16,17-octaethylporphycenato)tin(IV) [Sn^{IV}(OEPc)$(OH)_2$] (1).** Potassium carbonate (125 mg, 9.0×10^{-4} mol) and [Sn^{IV}(OEPc)Cl_2] (32 mg, 4.4×10^{-5} mol) were dissolved in a mixture of tetrahydrofuran (100 mL) and water (25 mL), then heated at reflux for 2 h. The solution was concentrated on a rotary evaporator to remove tetrahydrofuran, and the aqueous layer was extracted using dichloromethane. The organic layer was washed with water and then dried over anhydrous sodium sulfate and filtered, and then the solvent was removed to give the crude product, which was then recrystallized in dichloromethane/*n*-hexane which formed violet prism crystals (30 mg). Yield: 99%. UV−vis (in dichloromethane), [λ_{max}/nm] (ε/M^{-1} cm^{-1}): 396 (152 000); 615 (53 900); 628 (47 500). Anal. Calcd for $C_{36}H_{46}N_4O_2Sn \cdot CH_2Cl_2 \cdot H_2O$: C, 56.36; H, 6.39; N, 7.11. Found: C, 56.56; H, 6.29; N, 6.93. TOF-MS (MALDI): *m*/*z* [M − OH]$^+$, 669.19 ([M − OH]$^+$ calcd for 669.26). ^{1}H NMR ($CDCl_3$, 293 K): δ [ppm] 1.95−1.99 (m, 24H, $-CH_3$), 4.15−4.26 (m, 16H, β-CH_2−), 10.25 (s, 4H, methine).

***trans*-Bis(ferrocenecarboxylato)(2,3,6,7,12,13,16,17-octaethylporphycenato)tin(IV) [Sn^{IV}(OEPc)$(FcCOO)_2$] (2).** [Sn^{IV}(OEPc)$(OH)_2$] (10.4 mg, 1.52×10^{-5} mol) and ferrocenecarboxylic acid (7.1 mg, 3.08×10^{-5} mol) were dissolved in anhydrous dichloromethane (15 mL). The reaction mixture was refluxed at 42 °C for 24 h. The solution was filtered through a Celite pad. The solvent from the filtrate was evaporated to dryness. The residue was recrystallized in dichloromethane/*n*-hexane which formed violet prism crystals (9 mg). Yield: 54%. UV−vis (in dichloromethane), [λ_{max}/nm] (ε/M^{-1} cm^{-1}): 397 (192 000); 614 (67 000); 628 (59 000). Anal. Calcd for $C_{58}H_{62}N_4O_4Fe_2Sn \cdot 0.5CH_2Cl_2$: C, 60.99; H, 5.51; N, 4.86. Found: C, 61.35; H, 5.54; N, 5.01. TOF-MS (MALDI): *m*/*z* [M − Cl]$^+$, 881.37 ([M − Cl]$^+$ calcd for 881.25). ^{1}H NMR ($CDCl_3$, 293 K): δ [ppm] 1.92−2.01 (m, 24H, $-CH_3$), 2.00 (s, 4H, η^5-C_5H_4COO), 2.53 (s, 10H, η^5-C_5H_5), 3.06 (s, 4H, η^5-C_5H_4COO), 4.24−4.27 (m, 16H, β-CH_2−), 10.48 (s, 4H, methine).

***trans*-Dihydroxo(2,3,6,7,12,13,16,17-octaethylporphyrinato)tin(IV) [Sn^{IV}(OEP)$(OH)_2$] (3).** [Sn^{IV}(OEP)$(OH)_2$] (**3**) was prepared from [Sn^{IV}(OEP)Cl_2] in a manner similar to that previously reported.[26,27] Potassium carbonate (1.34 g, 9.7×10^{-3} mol) and [Sn^{IV}(OEP)Cl_2] (350 mg, 4.8×10^{-4} mol) were dissolved in a mixture of tetrahydrofuran (350 mL) and water (75 mL), then heated at reflux for 2 h. The solution was concentrated on a rotary evaporator to remove tetrahydrofuran, and the aqueous layer was extracted into dichloromethane. The organic layer was washed with water, dried over anhydrous sodium sulfate, and filtered, and then the solvent was removed

(22) Frisch, M. J.; Trucks, G. W.; Schlegel, H. B.; Scuseria, G. E.; Robb, M. A.; Cheeseman, J. R.; Montgomery, J. A., Jr.; Vreven, T.; Kudin, K. N.; Burant, J. C.; Millam, J. M.; Iyengar, S. S.; Tomasi, J.; Barone, V.; Mennucci, B.; Cossi, M.; Scalmani, G.; Rega, N.; Petersson, G. A.; Nakatsuji, H.; Hada, M.; Ehara, M.; Toyota, K.; Fukuda, R.; Hasegawa, J.; Ishida, M.; Nakajima, T.; Honda, Y.; Kitao, O.; Nakai, H.; Klene, M.; Li, X.; Knox, J. E.; Hratchian, H. P.; Cross, J. B.; Bakken, V.; Adamo, C.; Jaramillo, J.; Gomperts, R.; Stratmann, R. E.; Yazyev, O.; Austin, A. J.; Cammi, R.; Pomelli, C.; Ochterski, J. W.; Ayala, P. Y.; Morokuma, K.; Voth, G. A.; Salvador, P.; Dannenberg, J. J.; Zakrzewski, V. G.; Dapprich, S.; Daniels, A. D.; Strain, M. C.; Farkas, O.; Malick, D. K.; Rabuck, A. D.; Raghavachari, K.; Foresman, J. B.; Ortiz, J. V.; Cui, Q.; Baboul, A. G.; Clifford, S.; Cioslowski, J.; Stefanov, B. B.; Liu, G.; Liashenko, A.; Piskorz, P.; Komaromi, I.; Martin, R. L.; Fox, D. J.; Keith, T.; Al Laham, M. A.; Peng, C. Y.; Nanayakkara, A.; Challacombe, M.; Gill, P. M. W.; Johnson, B.; Chen, W.; Wong, M. W.; Gonzalez, C.; Pople, J. A. *Gaussian 03*; Gaussian, Inc.: Wallingford, CT, 2004.

(23) Williams, A. T. R.; Winfield, S. A.; Miller, J. N. *Analyst* **1983**, *108*, 1067.

(24) Fujitsuka, M.; Cho, D. W.; Tojo, S.; Inoue, A.; Shiragami, T.; Yasuda, M.; Majima, T. *J. Phys. Chem. A*. **2007**, *111*, 10574.

(25) (a) Gouterman, M.; Schwart, F. P.; Smith, P. D. *J. Chem. Phys*. **1973**, *59*, 676. (b) Iwamoto, H.; Hori, K.; Fukazawa, Y. *Tetrahedron* **2006**, *62*, 2789.

(26) Crossley, M. J.; Thordarson, P.; Wu, R. A.-S. *J. Chem. Soc., Perkin Trans*. **2001**, *1*, 2294.

(27) Arnold, D. P. *J. Chem. Educ*. **1988**, *65*, 1111.

Table 1. Crystallographic Data for **1**, **2**, **3**, and **4**

parameter	**1**	**2**	**3**	**4**
formula	$C_{37}H_{47}N_4O_2SnCl_3$	$C_{58}H_{62}N_4O_4SnFe_2$	$C_{37}H_{48}N_4O_2SnCl_2$	$C_{58}H_{62}N_4O_4SnFe_2$
fw	804.83	1109.51	770.38	1109.51
cryst syst	monoclinic	monoclinic	monoclinic	triclinic
space group	$P2(1)/c$	$P2(1)/n$	$P2(1)/n$	$P\bar{1}$
a/Å	8.8308(14)	14.203(7)	8.0026(16)	9.2134(10)
b/Å	26.249(4)	7.380(4)	10.502(2)	12.2298(13)
c/Å	9.3713(14)	23.318(11)	23.562(5)	13.5794(15)
α/deg	90	90	90	107.782(2)
β/deg	109.558(3)	91.460(9)°	90.636(3)	101.137(2)
γ/deg	90	90	90	92.321(2)
V/Å^3	2047.0(5)	2443(2)	1980.1(7)	1421.4(3)
Z	2	2	2	1
T/K	223(2)	100(2)	296(2)	100(3)
ρ_{calc}/g cm^{-3}	1.306	1.508	1.292	1.296
μ/mm^{-1}	0.854	1.146	0.815	0.985
reflns measured	10049	12111	9380	9752
unique reflns	2957	4280	2833	6445
R_{int}	0.0290	0.0753	0.0237	0.0201
observed data [$I > 2\sigma(I)$]	2559	3647	2490	5836
R_1[a], wR_2[b] [$I > 2\sigma(I)$]	0.0408, 0.1060	0.1149, 0.3104	0.0308, 0.0891	0.0362, 0.0981
$R1$ [a] wR_2[b] (all data)	0.0502, 0.1128	0.1256, 0.3164	0.0357, 0.0937	0.0404, 0.1014

[a] $R_1 = \sum||F_o| - |F_c||/\sum|F_o|$. [b] $wR_2 = [\sum w(F_o^2 - F_c^2)^2/\sum w(F_o^2)^2]^{1/2}$.

to give the crude product, which was then recrystallized in dichloromethane/*n*-hexane which formed red prism crystals (325 mg). Yield: 98%. UV−vis (in dichloromethane), [λ_{max}/nm] (ε/M^{-1} cm^{-1}): 407 (351 000); 537 (17 900); 574 (16 100). Anal. Calcd for $C_{36}H_{46}N_4O_2Sn \cdot 2CH_2Cl_2$: C, 53.36; H, 5.89; N, 6.55. Found: C, 54.12; H, 5.99; N, 6.58. TOF-MS (MALDI): m/z [M − OH]$^+$, 669.47 ([M − OH]$^+$ calcd for 669.26). ^{1}H NMR ($CDCl_3$, 293 K): δ [ppm] 2.03 (t, 24H, −CH_3), 4.20 (q, 16H, β-CH_2−), 10.47 (s, 4H, −CH−).

***trans*-Bis(ferrocenecarboxylato)(2,3,6,7,12,13,16,17-octaethylporphyrinato)tin(IV) [Sn^{IV}(OEP)(FcCOO)$_2$] (4).** [Sn^{IV}(OEP)(FcCOO)$_2$] (**4**) was prepared from [Sn^{IV}(OEP)(OH)$_2$] in a manner similar to that previously reported.[28] [Sn^{IV}(OEP)(OH)$_2$] (10.2 mg, 1.49×10^{-5} mol) and ferrocenecarboxylic acid (7 mg, 3.04×10^{-5} mol) were dissolved in anhydrous dichloromethane (15 mL). The reaction mixture was refluxed at 42 °C for 24 h. The solution was filtered through a Celite pad. The solvent from the filtrate was evaporated to dryness. The residue was recrystallized in dichloromethane/*n*-hexane which formed red prism crystals (16 mg). Yield: 97%. UV−vis (in dichloromethane), [λ_{max}/nm] (ε/M^{-1} cm^{-1}): 406 (396 000); 537 (17 500); 574 (16 500). Anal. Calcd for $C_{58}H_{62}N_4O_4Fe_2Sn \cdot 0.5C_6H_{14}$: C, 63.56; H, 6.03; N, 4.86. Found: C, 63.26; H, 5.92; N, 4.71. TOF-MS (MALDI): m/z [M − (FcCOO)]$^+$, 881.02 ([M − (FcCOO)]$^+$ calcd for 881.25). ^{1}H NMR ($CDCl_3$, 293 K): δ [ppm] 1.89 (s, 4H, η^5-C_5H_4COO), 2.03 (t, 24H, −CH_3), 2.48 (s, 10H, η^5-C_5H_5), 3.04 (s, 4H, η^5-C_5H_4-COO), 4.28 (q, 16H, β-CH_2−), 10.64 (s, 4H, −CH−).

X-Ray Crystallography. All crystals suitable for X-ray analyses were obtained by recrystallization at room temperature. The crystals were mounted on a glass fiber and used for the X-ray diffraction study. The measurements were made using a Bruker SMART APEX CCD detector with graphite-monochromated Mo Kα radiation (λ = 0.71073 Å) and a 2 kW rotating anode generator. The data were collected at 100 K to a maximum 2θ value of 28.28° in 0.30° oscillations. The data frames were integrated using SAINT (version 6.45) and merged to give a unique data set for the structure determination. Empirical absorption corrections by SADABS[29] were carried out. The structure was solved by a direct method and refined by the full-matrix least-squares method on all $F2$ data using the SHELX suite of programs.[30] The non-hydrogen atoms were anisotropically refined. The hydrogen atoms were included in the structure factor calculations, but not refined. The crystal data and details of the structure determinations are summarized in Table 1.

Results and Discussion

Syntheses and Structural Studies of Sn(IV) Porphyrinoid Complexes. The dihydroxy−Sn(IV) porphyrinoid complexes [Sn^{IV}(OEPc)(OH)$_2$], **1**, and [Sn^{IV}(OEP)(OH)$_2$], **3**, were obtained by treatment of the dichloro−Sn(IV) porphyrinoid complex with potassium carbonate in a mixture of tetrahydrofuran and water. The Sn(IV) porphyrinoid−ferrocene triad [Sn^{IV}(OEPc)(FcCOO)$_2$], **2** and [Sn^{IV}(OEP)(FcCOO)$_2$], **4**, were then synthesized by the reaction of the dihydroxy−Sn(IV) porphyrinoid complexes, **1** or **3**, with 2 equiv of ferrocenecarboxylic acid. All complexes were characterized by UV−vis, IR, ^{1}H NMR, MS, and elemental analysis, and their X-ray crystal structures were determined. These complexes showed parent ion peaks (**1**, 669.19 m/z; **2**, 881.37 m/z; **3**, 669.47 m/z; **4**, 881.02 m/z) resulting from the loss of one hydroxo or one ferrocenecarboxylate ligand under the MALDI-TOF mass spectral analysis conditions. In the IR measurement, the characteristic peak of **1** at 3621 cm^{-1} corresponding to the O−H stretching vibration of the hydroxyl group disappeared due to the ligand exchange reaction, and the alternative new peak of **2** at 1644 cm^{-1} attributed to the C=O stretch absorption of the ferrocenecarboxylate group was observed (Figure S2a, Supporting Information). For the Sn(IV) porphyrin complexes, the same spectral change was also observed (Figure S2b, Supporting Information).

All complexes afford a crystal suitable for X-ray analysis, and its molecular structures are shown in Figure 1.

(28) (a) Kim, H. J.; Jeon, W. S.; Lim, J. H.; Hong, C. S.; Kim, H.-J. *Polyhedron* **2007**, *26*, 2517. (b) Kim, H.-J.; Jo, H. J.; Kim, J.; Kim, S.-Y.; Kim, D.; Kim, K. *CrystEngComm*. **2005**, *7*, 417. (c) Kim, H. J.; Park, K.-M.; Ahn, T. K.; Kim, S. K.; Kim, K. S.; Kim, D.; Kim, H.-J. *Chem. Commun*. **2004**, 2594. (d) Smith, D.; Arnold, D. P.; Kennard, C. H. L.; Mak, T. C. W. *Polyhedron* **1991**, *10*, 509. (e) Liu, I.-C.; Lin, C.-C.; Chen, J.-H.; Wang, S.-S. *Polyhedron* **1996**, *15*, 459.

(29) Sheldrick, G. M. *SADABS*; University of Göttingen: Göttingen, Germany, 1996.

(30) Sheldrick, G. M. *SHELXL97*; *SHELXS97*; University of Göttingen: Göttingen, Germany, 1997.

Table 2. Bond Lengths (Å) and Bond Angles (deg) of **1**, **2**, **3**, and **4**

	1	2	3	4	[Sn(TPP)(FcCOO)$_2$][a]
Sn(1)−N(1)	2.087(3)	2.084(10)	2.099(3)	2.0858(19)	2.095(2)
Sn(1)−N(2)	2.083(3)	2.070(10)	2.101(3)	2.0902(19)	2.093(2)
Sn(1)−O(1)	2.046(3)	2.113(8)	2.033(2)	2.0731(16)	2.0730(16)
O(1)−Sn(1)−O(1A)	180.000(1)	180.0(5)	180.00(14)	180.000(1)	180.00(16)
O(1)−Sn(1)−N(2)	89.32(14)	86.8(4)	88.87(10)	82.80(7)	84.28(7)
O(1A)−Sn(1)−N(2)	90.06(14)	93.2(4)	91.13(10)	97.20(7)	95.72(7)
O(1)−Sn(1)−N(1A)	90.06(14)	94.5(4)	91.13(10)	86.74(7)	86.77(7)
O(1A)−Sn(1)−N(1A)	89.94(14)	85.5(4)	88.87(10)	93.26(7)	93.23(7)

[a] Data reported previously.[28a]

In the case of the dihydroxy−Sn(IV) porphyrinoid complexes, **1** and **3**, the distances of Sn(1)−N(1) (2.087(3) Å) and Sn(1)−N(2) (2.083(3) Å) for **1** are shorter than those of **3** (Sn(1)−N(1); that is, 2.099(3) Å, Sn(1)−N(2): 2.101(3) Å) as shown in Table 2. These results suggest that the electron density of Sn for **1** is higher when compared to **3** because the contribution of the lone-pair for nitrogen atoms may be greater in **1**. Therefore, the distance of Sn(1)−O(1) (2.046(3) Å) for **1** is slightly longer than that of the porphyrin complex, **3** (2.033(2) Å). Also, in the case of the Sn(IV) porphyrinoid−ferrocene complexes, **2** and **4**, it revealed the axially coordinated structure with a 1:2 stoichiometry of the Sn−porphycene (or porphyrin) and ferrocene moieties. The central Sn atom is octahedrally coordinated by the four pyrrole N atoms and two ferrocenecarboxylato units. Furthermore, the Sn atom lies on an inversion center, so that the two ferrocenecarboxylato units are oriented to the opposite side with respect to each other, similar to other carboxylato−Sn(IV) porphyrin complexes.[28] As for the bond length around the central Sn atom, as shown in Table 2, the distance of Sn(1)−O(1) (2.113(8) Å) for **2** is longer and the distances of Sn(1)−N(1) (2.084(10) Å) and Sn(1)−N(2) (2.070(10) Å) for **2** are shorter compared to those of the porphyrin complexes, **4** (Sn(1)−O(1); that is, 2.0731(16) Å; Sn(1)−N(1), 2.0858(19) Å; Sn(1)−N(2), 2.0902(19) Å) and Sn(TPP)(FcCOO)$_2$ (Sn(1)−O(1), 2.0730(16) Å; Sn(1)−N(1), 2.095(2) Å; Sn(1)−N(2), 2.093(2) Å),[28a] in which TPP denotes the 5,10,15,20-tetraphenylporphyrin ligand similar to the dihydroxy−Sn(IV) porphyrinoid complexes. Furthermore, the bond angle of O(1)−Sn(1)−N(2) (82.80(7)°) for **4** decreased when compared to **3** (88.87(10)°) by coordination of the ferrocenecarboxylic acid. This decrease in the bond angle for the Sn(IV) porphyrin complexes is greater than those of the Sn(IV) porphycene complexes (**1**, 89.32(14)°; **2**, 86.8(4)°). The straight line of O(1)−Sn(1)−O(1A) for **4** is inclined at *ca.* 80° to the Sn(IV) porphyrin mean plane. In contrast, the line of O(1)−Sn(1)−O(1A) for **2** intersects with the Sn(IV) porphycene mean plane almost perpendicular. Therefore, the center-to-center distance of **4** (5.711 Å) is shorter than that of **2** (5.844 Å).

Spectroscopic Properties of Sn(IV) Porphyrinoid−Ferrocene Complexes. Figure 2 shows the absorption spectra of the Sn(IV) porphyrinoid−ferrocene complexes in dichloromethane. The Soret and Q-bands of the complexes, **2** and **4**, were found to be similar to those of the corresponding dihydroxy complexes, **1** and **3**. These results suggest that there is no significant ground state electronic interaction between the Sn−porphycene (or porhyrin) and ferrocene units. Also, the Soret band intensities of **2** and **4** are hyperchromic (**2**, $\varepsilon = 1.9 \times 10^5$ M^{-1} cm^{-1}; **4**, $\varepsilon = 4.0 \times 10^5$ M^{-1} cm^{-1}) as compared to those of the dihydroxy complexes (**1**, $\varepsilon = 1.5 \times 10^5$ M^{-1} cm^{-1}; **3**,

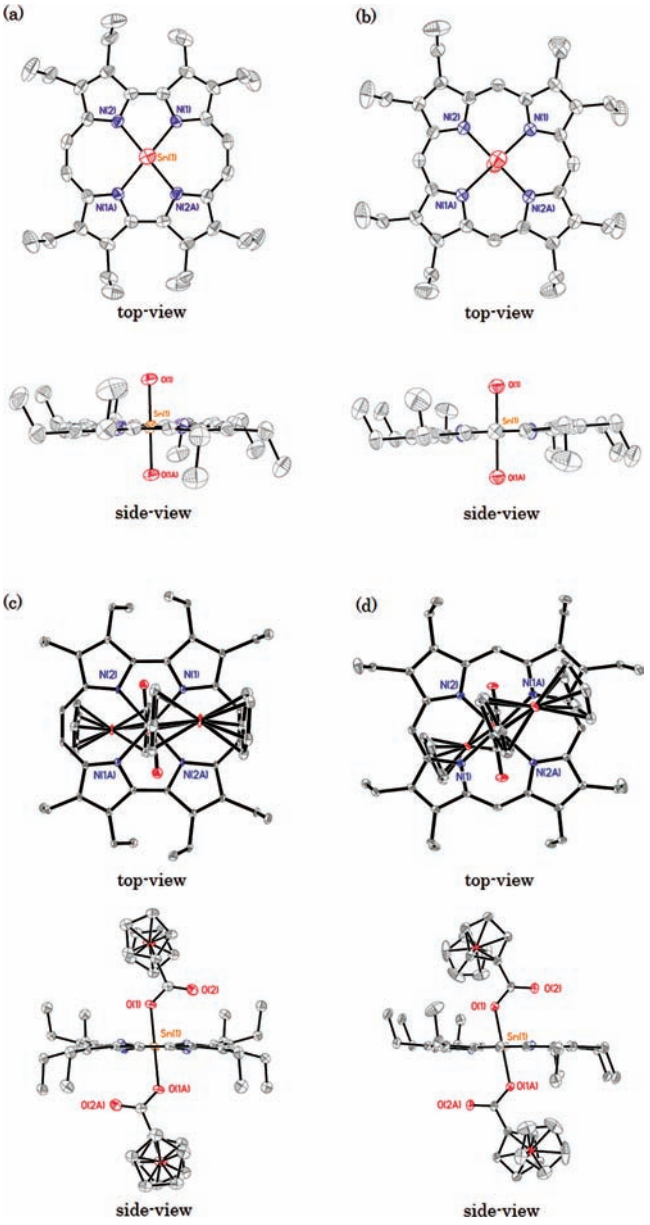

Figure 1. ORTEP drawing of Sn(IV) porphyrinoid complexes (a) **1**, (b) **3**, (c) **2**, and (d) **4** with thermal ellipsoids at 50% probability. The hydrogen atoms and the crystallization solvents have been omitted for clarity. The prime character in the labels indicates that these atoms are at equivalent positions (**1**, $1-x, 1-y, 1-z$; **2**, $2-x, 1-y, -z$; **3**, $1-x, 1-y, -z$; **4**, $1-x, 2-y, 1-z$).

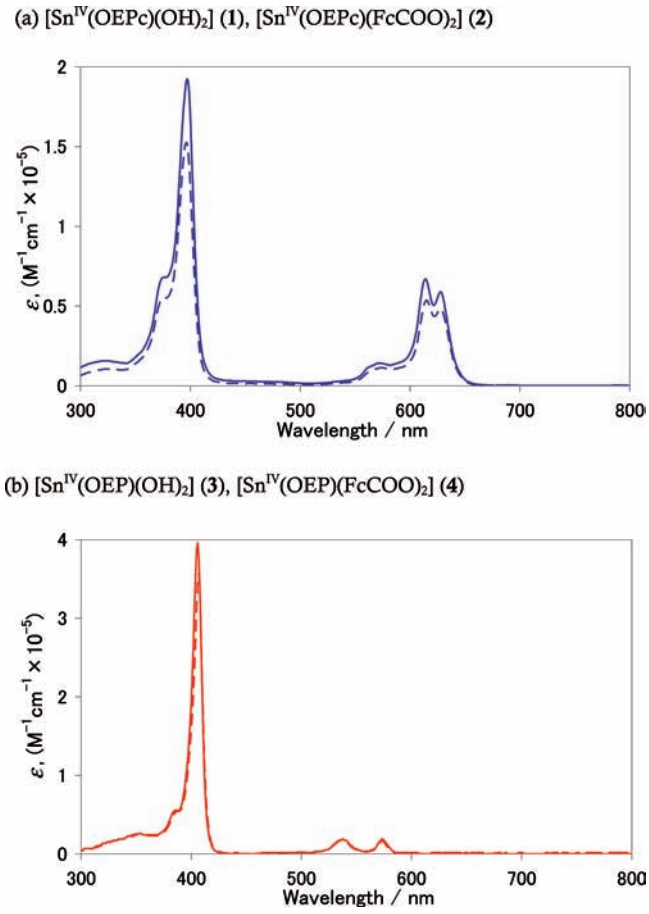

Figure 2. Steady-state UV−vis spectra of (a) **1** (dashed line) and **2** (solid line) and (b) **3** (dash line) and **4** (solid line) in dichloromethane.

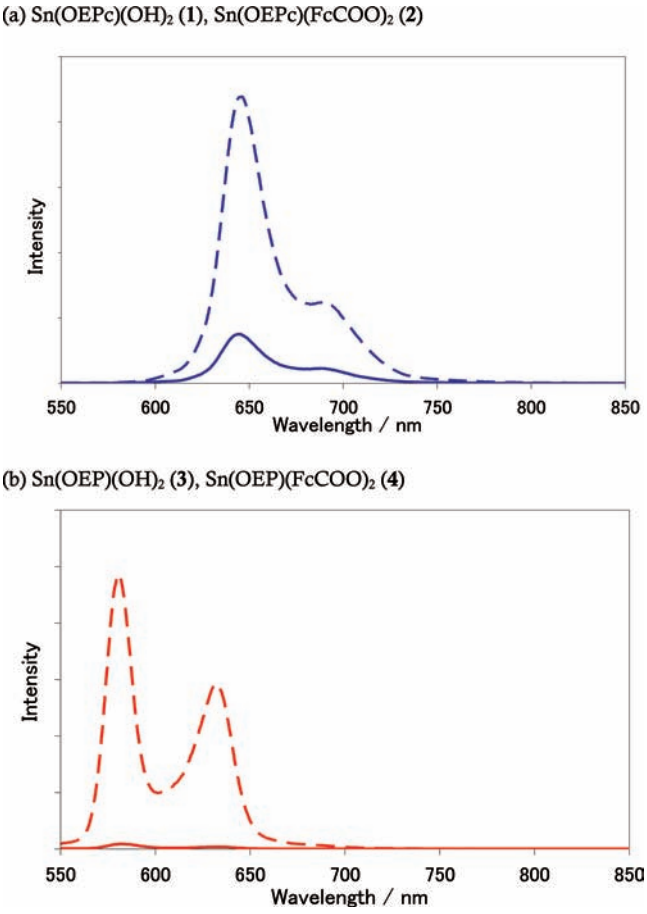

Figure 3. Fluorescence spectra of (a) **1** (dashed line) and **2** (solid line) and (b) **3** (dash line) and **4** (solid line) in dichloromethane. For the fluorescence measurements, the optical densities of the Sn(IV) complexes are adjusted to be the same at an excitation wavelength of 500 nm (abs. = 0.05).

$\varepsilon = 3.5 \times 10^5\ M^{-1}\ cm^{-1}$), indicating that the FcCOO unit more effectively causes some electronic perturbation of the porphycenato (or porphyrinato) ligand than the −OH probably due to a stronger charge transfer interaction.[31]

The steady-state fluorescence spectra of the Sn(IV) complexes were measured by adjusting the optical densities of the samples to be the same at the excitation wavelength of 500 nm. The fluorescence spectra of the Sn(IV) porphyrinoid−ferrocene complexes (solid line) were compared to the dihydroxy complexes (dash line) used as a reference in dichloromethane, as shown in Figure 3. The relative fluorescence intensities of both **2** and **4** are dramatically quenched by coordination of the ferrocenecarboxylic acid; in particulr, the emission of **4** was hardly observed. Also, as summarized in Table 3, the fluorescence quantum yields (Φ_F) of the Sn(IV) porphyrinoid−ferrocene complexes (**2**, $\Phi_F = 0.01$; **4**, $\Phi_F = < 0.001$) decreased compared to those of the dihydroxy complexes (**1**, $\Phi_F = 0.094$; **3**, $\Phi_F = 0.017$). The fluorescence quenching suggests that the PET from the ferrocene units to the excited singlet state generated by photoexcitaion because it is known that the excited Sn(IV) porphyrin works as a good electron acceptor.[32]

Table 3. Spectroscopic Data of Sn(IV) Complexes[a]

compound	λ_{abs}[b]/nm (10^{-4} ε/M^{-1} cm^{-1})	λ_{fluo}[c]/nm	Φ_F[c,d]
1	396(15.2), 615(5.39), 628(4.75)	645, 689(sh)	0.094
2	397(19.2), 614(6.70), 628(5.90)	645, 689(sh)	0.01
3	407(35.1), 537(1.79), 574(1.61)	581, 632	0.017
4	406(39.6), 537(1.75), 574(1.65)	581, 632	< 0.001

[a] λ_{abs}, absorption maximum; λ_{fluo}, fluorescence maximum. [b] Solvent, dichloromethane. [c] Solvent, toluene. [d] The absolute fluorescence quantum yield value of **1** was based on photoluminescent measurements using an integrating sphere with an excitation wavelength at 337 nm. The absolute fluorescence quantum yield values of **2**, **3**, and **4** were determined by the comparative method of Williams et al. where 2,7,12,17-tetra-*n*-propyl porphycene was used as the standard.[23]

Molecular Orbital Calculation. The molecular orbitals of the triad molecules, **2** and **4**, were estimated by molecular orbital calculations.[22] In this calculation, the ethyl groups of the porphycene (or porphyrin) were reduced to a methyl group for simplicity. Figure 4 shows the optimized molecular structure of **2**, and the pattern of the highest occupied molecular orbital (HOMO) and the lowest unoccupied molecular orbital (LUMO). For **2**, the HOMO is localized on the ferrocene. On the other hand, the LUMO of **2** is localized on the Sn(IV) porphycene. In the case of **4**, the HOMO and the LUMO are also localized on the ferrocene and Sn(IV) porphyrin, respectively (Figure S3, Supporting Information). These calculation results agreed

(31) Buchler, J. W. In *The Porphyrins*; Dolphin, D., Ed.; Academic Press: New York, 1978; Volume *I*, Chapter 10.
(32) (a) Jang, J. H.; Jeon, K.-S.; Oh, S.; Kim, H.-J.; Asahi, T.; Masuhara, H.; Yoon, M. *Chem. Mater.* **2007**, *19*, 1984. (b) Kadish, K. M.; Xu, Q. Y.; Maiya, G. B.; Barbe, J.-M.; Guilard, R. *J. Chem. Soc., Dalton Trans.* **1989**, 1531.

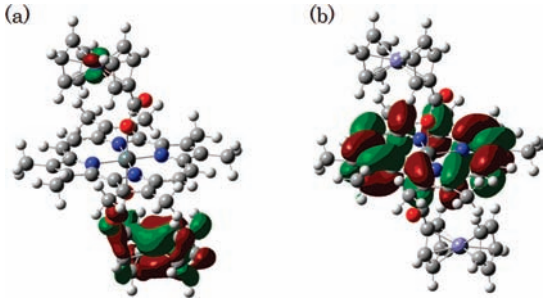

Figure 4. HOMO (left) and LUMO (right) orbital of **2** calculated by the DFT method at the B3LYP/3-21G* level using the Gaussian 03 package. The alkyl groups of [Sn^{IV}(OEPc)] were reduced to methyl groups.

with the redox behavior measured by cyclic voltammetry. As shown in Figure S4 (Supporting Information), the first reduction attributed to the Sn(IV) porphycene (or porphyrin) and the first oxidation assigned to the ferrocene/ferrocenium cation were observed. Therefore, this molecular orbital calculation was electrochemically supported, and the PET reaction from the ferrocene to Sn(IV) porphycene (or porphyrin) is expected when the Sn(IV) porphycene (or porphyrin) is excited.

Transient Absorption Spectrum. To directly detect the PET reaction, the transient absorption spectroscopy was applied to **1** and **2** in toluene and acetonitrile. These measurements were carried out by excitation of the sample by a 620 nm laser pulse. The obtained transient absorption spectra and time profiles of **2** in toluene and acetonitrile are shown in Figure 5a and b, respectively. In the present study, the ferrocenium cation band near 800 nm could not be detected because of its small molar extinction coefficient ($\varepsilon = \sim 10^3\ M^{-1}\ cm^{-1}$).[33] In the case of **1**, the porphycene radical anion species was not observed. Alternatively, a broad spectrum was obtained in the 800 to 1000 nm range (Figure S5, Supporting Information). This broad peak was nearly unchanged until 40 ps after the excitation. Therefore, this peak was attributed to the excited singlet state (S_1) because the fluorescence lifetime (τ_F) of **1** is ca. 5 ns.[34] In contrast, within 1 ps after excitation, the unique sharp peaks around 750 and 850 nm for the Sn(IV)−ferrocene complex, **2**, were observed in both toluene and acetonitrile. Because these peaks are similar to those reported for the [Sn^{IV}(TPrPc)] radical anion, in which TPrPc denotes the 2,7,12,17-tetra-*n*-propyl porphycene ligand,[14a] the generation of the radical anion of [Sn^{IV}(OEPc)] in Figure 5 can be attributed to the CS process. In toluene, the generated CS state decayed with two components, 3.9×10^{11} and $9.6 \times 10^9\ s^{-1}$ for time constants, as shown in Figure 5a. On the other hand, the generated CS state in acetonitrile disappeared with a single component with $6.9 \times 10^{11}\ s^{-1}$ for a time constant (Figure 5b).

Such a solvent dependence of the charge recombination (CR) process was reported when the fullerene (C_{60}) or porphyrins were used in the donor−acceptor system.[35] In this case, equilibrium between the CS state and the triplet (or singlet) state was taken into consideration. It is thus conceivable that these behaviors for the transient CS state of **2** are attributed to the equilibrium between the CS state and the triplet state (T_1) in toluene. On the other hand, in a polar solvent, such as acetonitrile, the energy level of the CS state became lower, and no equilibrium between the CS state and the triplet state (T_1) was established. Supporting this prediction, the driving force ($-\Delta G_{CS}$) for the PET from the excited singlet state was estimated. The driving force for the PET ($-\Delta G_{CS}$) in toluene and acetonitrile can be estimated using the following, Weller's equation:[36]

$$-\Delta G_{CS} = E_{red} - E_{ox} + E_{0-0} + \Delta G_s \qquad (1)$$

$$\Delta G_s = \frac{e^2}{4\pi\varepsilon_0}\left[\left(\frac{1}{2r_D}+\frac{1}{2r_A}\right)\left(\frac{1}{\varepsilon_s}-\frac{1}{\varepsilon_r}\right)-\frac{1}{\varepsilon_s R}\right] \qquad (2)$$

where E_{0-0} is the excitation energy of the excited singlet state (S_1) and E_{ox} and E_{red} are the first oxidation and first reduction potentials, respectively, in dichloromethane (Table 4). ΔG_S is the correction term that includes the effects of the solvent and the Coulombic interaction between the charged donor and acceptor. The values r_D and r_A are the radii of the charged donor and acceptor, respectively, and R is the center-to-center distance between them. The value ε_r is the dielectric constant of the solvent in which the redox potentials are determined (dichloromethane), and ε_s is the dielectric constant of the solvent used in the spectroscopic measurements (toluene or acetonitrile).[38] From these data, the driving forces (ΔG_{CS}) in toluene and acetonitrile were determined to be −0.44 and −1.13 eV, respectively.[15] The estimated energy level diagrams for **2** in toluene and acetonitrile are shown in Figure 6. Therefore, an equilibrium between the CS state and the triplet state (T_1) was proposed for the mechanism of the two-component decay because the energy level of the CS state is close to that of the triplet state (T_1) in toluene. Thus, for the two-component decay in toluene, the first component with $3.9 \times 10^{11}\ s^{-1}$ of time constant (k_{CR}^{I}) is attributed to the CR process from the CS state to the triplet state (T_1). On the other hand, the slow component with a $9.6 \times 10^9\ s^{-1}$ time constant (k_{CR}^{II}) is attributed to the CR process from the CS state to the ground state (S_0). Although the similar equilibrium of the CS state was reported for several donor−acceptor

(33) Kubo, M.; Mori, Y.; Otani, M.; Murakami, M.; Ishibashi, Y.; Yasuda, M.; Hosomizu, K.; Miyasaka, H.; Imahori, H.; Nakashima, S. *J. Phys. Chem. A* **2007**, *111*, 5136.

(34) The fluorescence lifetime (τ_S) of **1** was determined using a streak camera (Hamamatsu C4780) with a laser diode (LD; λ = 375 nm, pulse width ~200 ps, and repetition rate ~100 MHz) as the excitation source: τ_S = 4981 ps.

(35) (a) Fujitsuka, M.; Ito, O.; Yamashiro, T.; Aso, Y.; Otsubo, T. *J. Phys. Chem. A* **2000**, *104*, 4876. (b) Yamazaki, M.; Araki, Y.; Fujitsuka, M.; Ito, O. *J. Phys. Chem. A* **2001**, *105*, 8615. (c) Komamine, S.; Fujitsuka, M.; Ito, O.; Moriwaki, K.; Miyata, T.; Ohno, T. *J. Phys. Chem. A* **2001**, *105*, 11497. (d) Asahi, T.; Ohkohchi, M.; Matsusaka, R.; Mataga, N.; Zhang, R. P.; Osuka, A.; Maruyama, K. *J. Am. Chem. Soc.* **1993**, *115*, 5665. (e) Osuka, A.; Marumo, S.; Mataga, N.; Taniguchi, S.; Okada, T.; Yamazaki, I.; Nishimura, Y.; Ohno, T.; Nozaki, K. *J. Am. Chem. Soc.* **1996**, *118*, 155.

(36) Weller, A. *Z. Phys. Chem. Neue Folge.* **1982**, *133*, 93.

(37) (a) Mataga, N.; Chosrowjan, H.; Taniguchi, S.; Shibata, Y.; Yoshida, N.; Osuka, A.; Kikuzawa, T.; Okada, T. *J. Phys. Chem. A* **2002**, *106*, 12191. (b) It was reported that eq 2 gives too high ΔG_S values in nonpolar solvents, such as toluene. The calculated ΔG_S value decreased by 0.35 eV as indicated in ref 37a.

(38) Dean, J. A. In *Lange's Handbook of Chemistry*, 15th ed.; McGraw-Hill: New York, 1999.

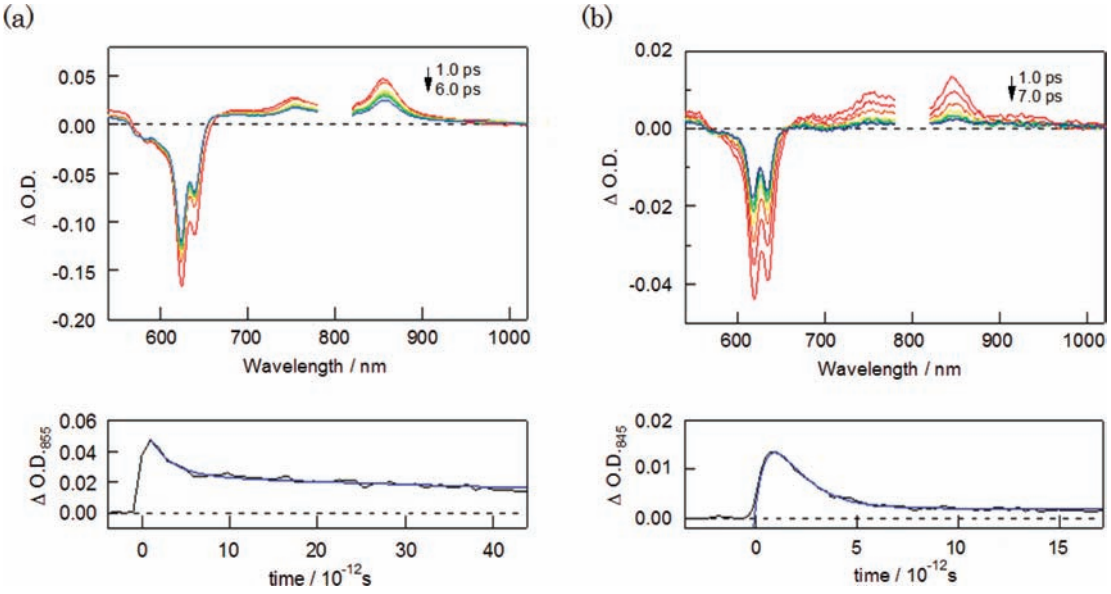

Figure 5. Transient absorption spectra of **2** in (a) toluene and (b) acetonitrile during the laser flash photolysis using a 620 nm femtosecond pulse for excitation. The spectra were obtained at intervals of 1 ps after the laser excitation. The lower panel is a kinetic trace of ΔO.D. at 845 nm during the laser flash photolysis. The blue curve is the fitted curve.

Table 4. Redox Potentials and Driving Force ($-\Delta G_{CS}$) of **2** and **4** in Toluene and Acetonitrile

	E_{red}[a]	E_{ox}[a]	E_{0-0} (eV)[b]		E_T (eV)[c]	$-\Delta G_{CS}$ (eV)[d]	
compound	(vs SCE)	(vs SCE)	toluene	acetonitrile		toluene	acetonitrile
2	−0.84	0.49	1.95	1.98	1.31	0.44	1.13
4	−1.36	0.48	2.14	2.16	1.74	0.15	0.81

[a] Redox potentials were measured by cyclic voltammetry in dichloromethane (Figure S4, Supporting Information). [b] E_{0-0} is the excitation energy of the excited singlet state. [c] E_T is the energy of the excited triplet state, and its values were estimated by phosphorescence in bromobenzene (Figure S6, Supporting Information). [d] The listed values were calculated using 2 Å as r_D. r_A values for [Sn^{IV}(OEPc)] and [Sn^{IV}(OEP)] were 5 Å.[15] *R* values for **2** and **4** were 5.844 and 5.711 Å, respectively. $-\Delta G_{CS}$ in toluene solutions was calculated by means of the corrected ΔG_S value, which was decreased by 0.35 eV according to previous method.[15,33,37]

systems using porphyrins,[35d,e] all of these equilibriums took place between the CS state and the singlet state (S_1) of the porphyrins. To the best of our knowledge, no equilibrium with the triplet state (T_1) of the porphyrins was reported. Furthermore, such an equilibrium for the CS state is the first to be reported for a donor−acceptor system using metalloporphycene.

The PET reaction of **2** was compared to that of a Sn(IV) porphyrin having the same substituent and axial ligand, **4**. The transient absorption measurement of **4** was carried out by excitation of the sample with a 540 nm laser pulse in toluene and acetonitrile. After excitation, the transient species attributed to the radical anion of [Sn^{IV}(OEP)] was observed within 1 ps. The obtained CS states in both toluene and acetonitrile decayed with 1.2×10^{12} and 1.7×10^{11} s^{-1} time constants, respectively, as shown in Figure 7. However, in the case of **4**, no equilibrium similar to **2** was observed. As shown in Table 4, the estimated driving force ($-\Delta G_{CS}$, 0.15 eV) for the PET from the excited singlet state (S_1) indicated that the CS state is difficult to establish an equilibrium with along with the triplet state (T_1) due to the small driving force ($-\Delta G_{CS}$) and large energy gap between the CS state and triplet state (T_1) in toluene. It is conceivable that this difference in the driving force ($-\Delta G_{CS}$) is attributed to the porphycene skeleton. In the present study, E_{ox} and E_{0-0} of Sn(IV) porphycene−ferrocene, **2**, were comparable to the Sn(IV) porphyrin−

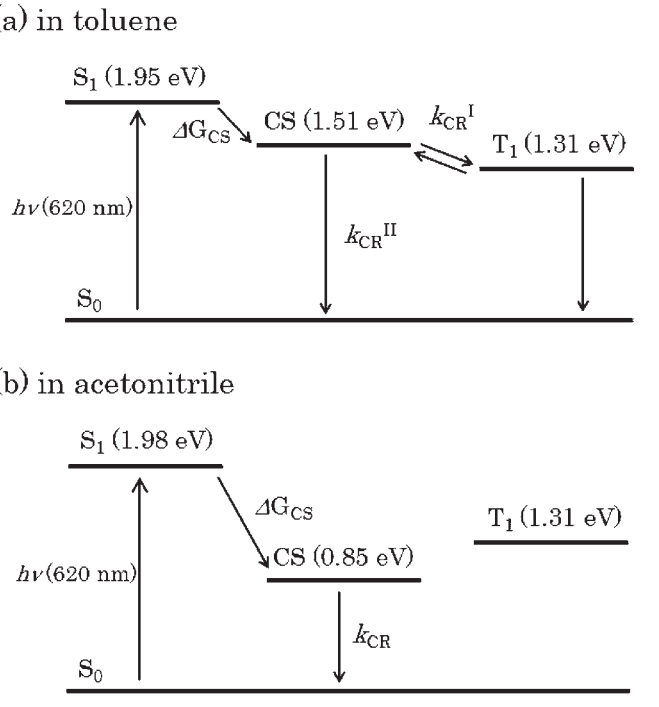

Figure 6. Energy diagram of Sn−ferrocene complex **2** (a) in toluene (nonpolar solvent) and (b) acetonitrile (polar solvent). Numbers indicate energy levels in eV units relative to the ground state (S_0).

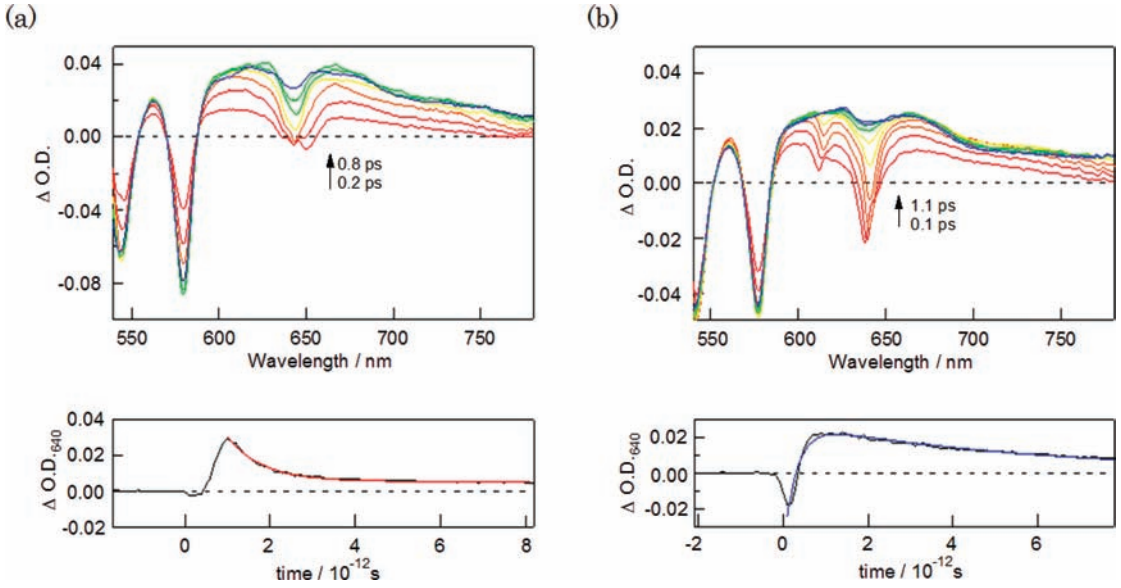

Figure 7. Transient absorption spectra of **4** in (a) toluene and (b) acetonitrile during the laser flash photolysis using 540 nm femtosecond pulse for excitation. The spectra were obtained at intervals of 0.1 ps after the laser excitation. The lower panel is a kinetic trace of ΔO.D. at 640 nm during the laser flash photolysis. The blue curve is the fitted curve.

ferrocene, **4**. However, the porphycene ring reduction was shifted more positive compared to **4** by the significant stabilization of the LUMO energy level with a decrease in the symmetry of the tetrapyrrolic macrocycle (Figure S4, Supporting Information). As a result, the driving force ($-\Delta G_{CS}$) of **2** becomes larger than those of **4** due to the property that is more readily reduced, and then the CS state is stabilized. Therefore, it is expected that porphycenes are some excellent candidates as electron acceptors because the porphycene ring is more readily reduced.

Conclusion

The molecular devices consisting of porphyrin or the nonporphyrin tetrapyrrolic macrocycle were attractive for the development and design of novel artificial photosynthesis and applications in molecular electronic devices. In this study, we synthesized a novel Sn(IV) porphycene−ferrocene triad molecule and investigated its PET behavior by subpicosecond laser flash spectroscopy, which revealed the formation of the Sn(IV) porphycene radical anion species. The generated CS state specifically decayed with a two-component time constant in a nonpolar solvent such as toluene. On the other hand, the CS state disappeared in one step in a polar solvent such as acetonitrile. The CR processes in these solvents can be explained on the basis of the driving force ($-\Delta G_{CS}$). Therefore, it became clear that there is a considerable equilibrium between the CS state and the triplet state (T_1) because these energy levels are close in toluene. The same equilibrium for the CR process was not observed in the Sn(IV) porphyrin having the same substituent and axial ligand. This result indicated that the driving force ($-\Delta G_{CS}$) of the Sn(IV) porphycene−ferrocene is larger than those of the Sn(IV) porphyrin−ferrocene. Therefore, it was suggested that, by using porphycene as an electron acceptor, the CS state is more stabilized compared to the porphyrin.

Acknowledgment. This study was supported by a Grant-in-Aid for Scientific Research on Priority Areas (No. 460, "Chemistry of Concerto Catalysis"); the Global COE Program "Science for Future Molecular System" from the Ministry of Education, Culture, Sports, Science and Technology of Japan (MEXT); a Grant-in-Aid for Scientific Research (20.02314) and a Grant-in-Aid for Scientific Research (A) (No. 21245016) from the Japan Society for the Promotion of Science (JSPS).

Supporting Information Available: The crystallographic data in CIF format. The comparative fluorescence quantum yields of **2**, **3**, and **4** (Figure S1). IR spectra of **1**, **2**, **3**, and **4** (Figure S2). Molecular orbital calculation of **4** (Figure S3). Cyclic voltammograms of **2** and **4** (Figure S4). Transient absorption spectrum of **1** (Figure S5). Phosphorescence spectra of **2** and **4** (Figure S6). This material is available free of charge via the Internet at http://pubs.acs.org.